JVSTB
JOURNAL OF VACUUM SCIENCE AND TECHNOLOGY B

Area selective atomic layer deposition of titanium dioxide: Effect of precursor chemistry

Ashwini Sinha, Dennis W. Hess, and Clifford L. Henderson

Citation: J. Vac. Sci. Technol. B **24**, 2523 (2006); doi: 10.1116/1.2359728
View online: http://dx.doi.org/10.1116/1.2359728
View Table of Contents: http://avspublications.org/resource/1/JVTBD9/v24/i6
Published by the AVS: Science & Technology of Materials, Interfaces, and Processing

Area selective atomic layer deposition of titanium dioxide: Effect of precursor chemistry

Ashwini Sinha, Dennis W. Hess, and Clifford L. Henderson[a)]
School of Chemical and Biomolecular Engineering, Georgia Institute of Technology, 311 Ferst Drive N.W., Atlanta, Georgia 30332-0100

(Received 17 May 2006; accepted 6 September 2006; published 30 October 2006)

Area selective atomic layer deposition (ALD) of titanium dioxide using polymer films as masking layers has been investigated. A number of factors which must be considered while designing a successful area selective ALD process have been determined and are briefly discussed. Reactivity of the polymer with the ALD precursor species, diffusion of ALD precursors through the polymer mask, and remnant precursor content in the masking film during ALD cycling are key factors. This article investigates the effect of different precursor chemistries in view of the above mentioned factors. Titanium tetrachloride and titanium isopropoxide have been used as two different metal precursors in conjunction with poly(methyl methacrylate) films as photodefinable masking layers. Processing problems arising from factors such as diffusion of precursors through the masking layer can be solved through careful choice of ALD precursors. © *2006 American Vacuum Society.*
[DOI: 10.1116/1.2359728]

I. INTRODUCTION

Atomic layer deposition (ALD) has become an important technique for depositing high quality ultrathin films.[1,2] ALD relies on an alternating cycle of exposures of a surface to two or more precursors that result in self-limiting surface reactions. Each subsequent surface reaction occurs only on the reactive sites produced by reagents in the preceding cycle, and in this way the desired film is built up essentially one atomic layer at a time. This method is particularly well suited for producing extremely thin, high quality, conformal films with thicknesses in the 3–10 nm range where other deposition techniques such as chemical vapor deposition have significant limitations. During ALD, film growth depends critically on the chemistry of the surface upon which each deposition cycle reaction occurs. Therefore, it should be possible to chemically tailor a surface to achieve area selective deposition. Selective ALD requires that designated areas of a surface be masked or "protected" to prevent ALD reactions in those selected areas, thus ensuring that the ALD film nucleates and grows only on the desired unmasked regions. There are many potential advantages to such an area selective atomic layer deposition technique (ASALDT) including elimination of etch processes for film patterning, reduction in the number of cleaning steps required, and patterning of materials which are difficult to etch.

The possibility of performing selective ALD has been pursued extensively in recent years.[3–10] Early ASALDT approaches involved the use of reactive compounds, such as alkyl silanes (e.g., alkyl trichlorosilanes, alkyl triethoxysilanes, etc.), as surface modifying agents. The concept in that work was to chemically convert sites on the substrate surface which would be reactive toward the ALD precursors into a nonreactive form and thus prevent ALD nucleation and growth. For example, chlorosilane compounds were chemically reacted to convert active hydroxyl sites on a substrate to relatively unreactive alkyl compounds. In particular, deposition of self-assembled monolayers (SAMs) of octadecyltrichlorosilane has been widely investigated as a method of surface modification to block the nucleation and ALD growth of a variety of inorganic films including ZnO, TiO_2, HfO_2, and ZrO_2.[3–5,7] Some of these previous studies observed that the SAM film must be defect-free in order to produce successful patterning, otherwise ALD precursors can easily access active sites available at the defects and cause undesired nucleation in the protected regions.[4,8,10] Unfortunately, achieving a defect-free SAM is extremely difficult and generally requires extended SAM deposition times. Such long and unreliable masking layer deposition techniques do not lend themselves to simple, inexpensive, or industrially practical processes. In addition, patterning of traditional SAMs relies on relatively nonstandard lithographic techniques, such as microcontact printing, and these lithographic methods are not conducive to the formation of defect-free patterned films and are in general not practical for current industrial applications. All of these issues pose serious limitations to the achievement of successful commercial applications of SAM-based area selective ALD processes.

In order to overcome these limitations encountered with SAM-based masking schemes, methods and materials for producing nonreactive, defect-free thin masking films are required. Furthermore, one can extend the masking concept beyond the idea that active sites on the substrate must be chemically protected from subsequent ALD reactions to include schemes in which the reactive sites are simply physically protected or screened from reaction. Considering these issues, the authors have recently proposed that polymer films present an opportunity to quickly and easily form defect-free ALD masking layers which rely primarily on physical screening of active sites on the substrate surface to enable

[a)]Author to whom correspondence should be addressed; electronic mail: cliff.henderson@chbe.gatech.edu

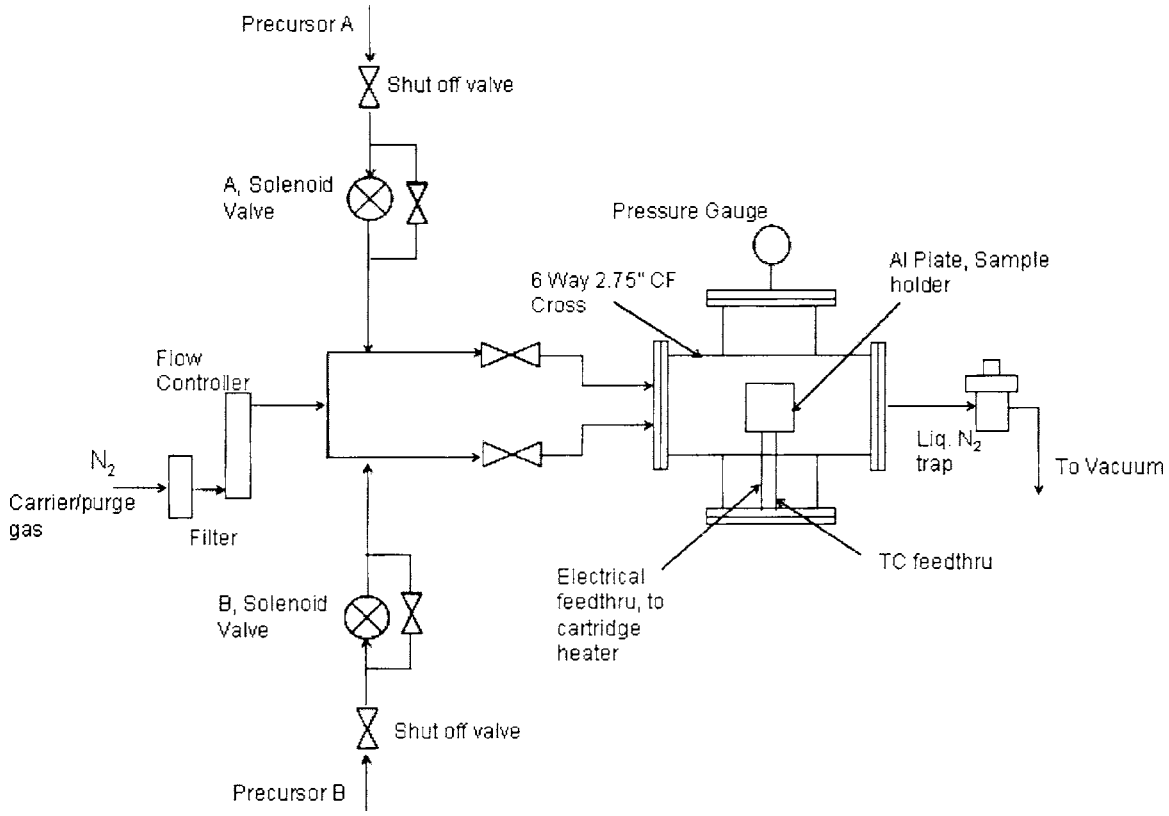

FIG. 1. Schematic of the ALD reactor.

area selective ALD.[8,10] In fact, polymer thin film properties such as ease of coating, high film quality, and access to a variety of material chemistries have led to the fact that polymer films are exploited as masking layers in the vast majority of all modern microlithography processes. As a result, a significant amount of research has been invested in developing a variety of different polymeric materials for high resolution patterning, including polymers based on epoxies, cresol resins (i.e., novolac polymers), poly(hydroxystrene), poly(norbornene), polyacrylates, polyimides, and polycarbonates. Thus, if a polymer or class of polymers can be identified that can prevent the nucleation and growth of a material on its surface during ALD, and which can be conveniently patterned using optical or other current lithographic methods, then such lithographically defined patterned polymer films can be used as deposition templates for area selective ALD. A "photoresist-like" process should offer a significantly better alternative as an ASALDT compared to SAM-based approaches and could facilitate rapid adoption of such methods into industrial practice. After ALD is completed, the goal is easy removal of the polymer masking layer in the same way that resist films are stripped, thus obtaining a direct patterned structure of the desired ALD film. As a first step toward this goal of developing polymer masking ASALDT (PM-ASALDT) approaches, the authors recently reported the successful area selective ALD of TiO_2 on Si substrates using $TiCl_4$ and de-ionized (DI) water as precursors and poly(methyl methacrylate) (PMMA) as a photodefinable masking layer.[10] However, several limitations of this ASALDT process were discovered which were due to a combination of the intrinsic reactivity of PMMA with $TiCl_4$ and the diffusion of $TiCl_4$ through the PMMA film. For example, it was discovered that a minimum masking layer thickness of approximately 180 nm was required to prevent undesired titania formation beneath the PMMA polymer mask. It was also discovered that the PMMA film was difficult to remove using simple solvent washes after ALD, and this difficulty was attributed to reaction of the $TiCl_4$ precursor with the PMMA film. Such limitations are of course undesirable, and thus further investigations of the influence of process conditions, precursor chemistry, and masking layer chemistry on the resulting ASALDT process performance were undertaken. In this work, titanium isopropoxide (TiIP) has been used as an alternate titanium precursor and the results of using the TiIP–H_2O system with PMMA masking layers are compared to the earlier work on the $TiCl_4$–H_2O–PMMA system. Results demonstrate that a PM-ASALDT process based on TiIP–H_2O–PMMA overcomes the limitations of the $TiCl_4$-based process and greatly enhances the PM-ASALDT process window for deposition of TiO_2 ultrathin films.

II. EXPERIMENTAL APPARATUS AND PROCEDURE

Figure 1 presents a schematic of the experimental apparatus used to perform ALD. The ALD system consists of a six-way 2.75 in. conflat cross which serves as the reaction chamber. Samples are placed onto an aluminum plate which

is instrumented with a *K*-type thermocouple for temperature measurement and can be heated using 1 in. CSH series cartridge heaters. Ultrahigh purity nitrogen is supplied through a rotameter and mixes with the ALD precursors before entering the reaction chamber. Nitrogen serves as both the carrier gas and purge gas for this ALD system. The chamber is evacuated with an Alcatel 2021SD rotary vane pump; chamber pressure is controlled by simultaneously varying the conductance of the pump via a throttle valve and the flow rate of nitrogen. Maximum conductance is used in order to achieve the maximum flow rate of nitrogen purge through the system. ALD is performed at a total pressure of 1 Torr with a total N_2 flow rate of 78 SCCM (SCCM denotes cubic centimeter per minute at STP). Pressure inside the chamber is monitored using a thermocouple-based vacuum pressure gauge connected to one port of the six-way cross. Precursors are introduced into the chamber in an alternating manner by using computer controlled solenoid valves. A metering valve is also attached immediately upstream of each solenoid valve in order to control the total flow rate of each precursor. A liquid nitrogen trap placed between the chamber and vacuum pump prevents unreacted precursors and products from entering the pump.

Blanket film depositions were initially conducted in order to investigate system behavior and determine the operating conditions required to perform ALD using both the titanium tetrachloride-water precursor system and the titanium isopropoxide-water precursor system for the deposition of TiO_2. Titanium tetrachloride ($TiCl_4$, 99.9%) was purchased from Sigma-Aldrich and used as received. Titanium isopropoxide (TiIP, 98%) was received from Dupont and was degassed using a series of freeze-pump-thaw cycles before use. DI water was used as the oxygen precursor source. $TiCl_4$ and water were maintained at approximately 25 °C while the titanium-isopropoxide precursor was heated to 82 °C to increase its vapor pressure. During titanium-isopropoxide depositions, all flow lines containing the precursor were also heated in order to avoid condensation of the precursor. All depositions were conducted at a substrate temperature of 160 °C and 1 Torr chamber pressure. *p*-type silicon ⟨100⟩ wafers were used as substrates. Wafers were thoroughly rinsed with acetone, methanol, isopropanol, and DI water to remove surface organics and then immersed in 2*M* HNO_3 for 2 h to increase the surface hydroxyl concentration before ALD.[11] After removal from the HNO_3 solution, the wafers were rinsed again with DI water and dried under nitrogen before being loaded into the ALD chamber. ALD was started after each sample had been loaded into the ALD chamber under N_2 purge and then evacuated for 2 h. This long evacuation time ensured complete removal of undesired volatile compounds in the chamber and from all flow lines. The base pressure of the chamber was maintained at 20 mTorr during this evacuation. The ALD cycle used consisted of (1) $TiCl_4$ or TiIP pulse, (2) N_2 purge, (3) H_2O pulse, and (4) N_2 purge. PMMA films were spin coated onto Si wafers from a 1–5 wt % PMMA (Scientific Polymer Products, M_W =54,000) polymer solution in toluene. The samples were soft baked at 120 °C for 5 min on a hot plate and then vacuum annealed at 100 °C for 2 h to ensure removal of residual casting solvent.

A. Film thickness measurements

Film thicknesses were measured using both spectroscopic ellipsometry and x-ray reflectivity. Spectroscopic ellipsometry measurements were performed with an M-2000 ellipsometer (J.A. Woollam Co. Inc.). Ellipsometry data were collected over a wavelength range from 400 to 1000 nm at angles of 65°, 70°, and 75° (with respect to the normal to the substrate plane). Data were analyzed to determine both film thickness and refractive index using the WVASE-32 software package (J.A. Woollam Co.) by employing a Cauchy model for the films and using a standard silicon substrate library data file. X-ray reflectivity measurements were performed using an X'PERTPRO x-ray diffraction system (PANalytical Inc.). For x-ray reflectivity experiments, copper radiation (wavelength of 1.54 Å) was used with the x-ray source generator tension and current set at 45 kV and 40 mA, respectively. Samples were scanned at low incident angles from 0° to 3.0° with a step size of 0.005° and a time per step of 0.1 s. Data were analyzed using the X'PERT reflectivity software which calculates the film thickness from the relative distance in angular position of the fringes in the reflectivity scans. Thicknesses measured using both techniques generally agreed to within ±0.2 nm.

B. X-ray photoelectron spectroscopy (XPS)

Chemical analysis of the films and surfaces was performed using XPS. XPS spectra were collected using a Physical Electronics (PHI) model 1600 XPS system equipped with a monochromator. The system used an Al $K\alpha$ source ($h\nu$=1486.8 eV) operating at 350 W beam power. Ejected photoelectrons were detected by a hemispherical analyzer that provided both high sensitivity and resolution. The operating pressure in the sampling chamber was below 5×10^{-9} Torr. Samples were aligned in the beam by maximizing photoelectron counts corresponding to the primary C 1*s* peak in C–C bonds located at a binding energy of 284.8 eV. A neutralizer beam was used during XPS measurements to compensate for peak shifting which occurs due to charging of samples during x-ray exposure. All high resolution spectra were collected using a pass energy of 46.95 eV. The step size and time per step were chosen to be 0.025 eV and 100 ms, respectively. Atomic concentrations of different elements were calculated based on the photoelectron intensities of each element and the elemental sensitivity factors provided by the tool manufacturer. Samples were scanned at different locations and the peak intensity and composition at different locations were compared to assure uniformity of film composition over the sample surface. XPS spectra showed that the deposited titania films are generally free of contaminants to the level of detectability (~0.1 at. %). Titanium concentrations on the surface are of particular impor-

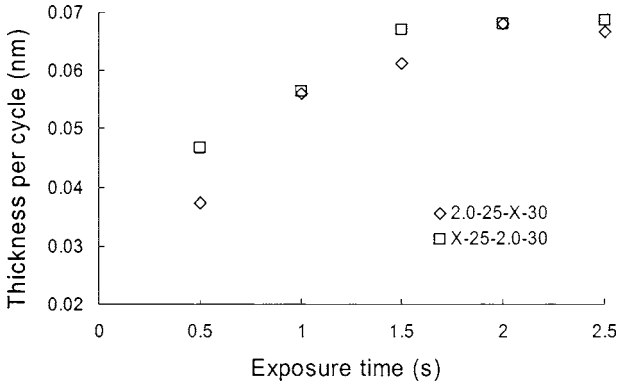

FIG. 2. Thickness grown per ALD cycle vs exposure time for one of the ALD precursors. The legend format refers to the time duration of each step in the ALD cycle. For example, *X*–25–2.0–30 refers to an ALD sequence of (1) *X* s exposure of $Ti[OCH(CH_3)_2]_4$, (2) 25 s N_2 purge, (3) 2.0 s exposure to water, and (4) 30 s N_2 purge. The two different data sets are for varying the (□) $Ti[OCH(CH_3)_2]_4$ exposure time and the (◇) water exposure time.

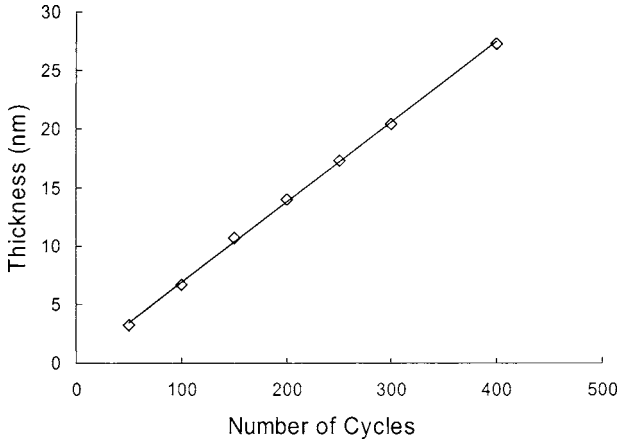

FIG. 3. Thickness of the TiO_2 film as a function of the number of ALD cycles. The linear growth with number of cycles is indicative of an ALD process.

tance in this work; thus, the titanium signals were analyzed using the Ti 2*p*3 peak at 458.8 eV (see Fig. 6) which is characteristic of titanium in TiO_2.[12]

III. RESULTS

A. Deposition on Si substrate

The growth rate data for ALD of TiO_2 films using $TiCl_4$ and H_2O as precursors have been published elsewhere.[10] Figure 2 shows the growth rate of TiO_2 films using the titanium-isopropoxide precursor as a function of varying precursor pulse duration for one of the precursors while maintaining a constant pulse time for the other precursor. The data suggest self-saturated reaction and growth of TiO_2 films at precursor exposure times for Ti isopropoxide and water of at least 1.5 and 2.0 s, respectively at 160 °C. Under these conditions, the growth rate of TiO_2 saturates at ~0.068 nm/cycle. The growth also exhibits the characteristic ALD behavior that the deposited film thickness is linearly proportional to the number of ALD cycles (see Fig. 3). The data presented in Figs. 2 and 3 clearly demonstrate self-saturated ALD growth of TiO_2. Previous studies[13] investigating the reaction mechanism of the titanium isopropoxide-water ALD process also reported that similar precursor exposure pulse durations were required for saturated growth at 150 °C. However, previous literature reports for the TiO_2 growth rate using the TiIP–H_2O precursor system exhibit some contradictory results. Doring *et al.*[14] measured a growth rate of 0.15 nm/cycle at 150 °C, while Ritala *et al.* reported a growth rate of only 0.015 nm/cycle at the same substrate temperature.[15] Recent studies have reported more consistent growth rates in the range of 0.05–0.06 nm/cycle at temperatures of 200–250 °C (Ref. 16) and 0.068 nm/cycle at 150 °C.[7] The growth rate obtained in this work appears to be in good agreement with these more recent studies.

Comparison of the TiIP–H_2O data with the previous $TiCl_4$ process[10] indicates that a slightly shorter titanium precursor pulse time is required for self-saturated growth in the case of the TiIP process (~1.5 s) as compared to the $TiCl_4$ (≥2.5 s) process. In both cases, a similar water pulse time of approximately 2 s is sufficient to achieve self-saturated growth. However, titania growth rates for both the TiIP (0.068 nm/cycle) and $TiCl_4$ (0.07 nm/cycle) processes are essentially the same. One marked difference between the isopropoxide and chloride precursors is the ligand size of the leaving group. Titanium isopropoxide is a significantly larger molecule than $TiCl_4$. Also, reaction mechanism studies on the TiIP–H_2O ALD process indicate that at 150–200 °C, two ligands per titanium-isopropoxide molecule are released during the exchange reaction with a hydroxylated surface, whereas $TiCl_4$ reacts with either one or two hydroxyl groups under the same conditions.[13,16–19] Therefore, on average, one TiIP molecule reacts with a larger number of hydroxyl groups on the surface than does one $TiCl_4$ molecule. This larger consumption of hydroxyl sites, combined with the larger steric hindrance of the remaining ligands on the TiIP molecule, leads to a lower number of TiIP molecules saturating the substrate surface compared to that for $TiCl_4$. Such considerations may partially explain the faster saturation of the surface by titanium isopropoxide during the titanium precursor pulse. If indeed a lower number of titanium molecules are deposited per layer, then a density difference between titania deposited using TiIP versus $TiCl_4$ might be expected. Spectroscopic ellipsometry measurements showed that the refractive indices of titania films made using the $TiCl_4$ precursor were in the range of 2.15–2.30 while the refractive indices for films made using the TiIP precursor were in the range of 2.10–2.20 (refractive indices reported at a wavelength of 580 mm). Since refractive index is an indicator of film density for a specific material composition, it can be inferred that the TiO_2 films obtained using the isopropoxide precursor process are indeed slightly less dense than those obtained using the chloride precursor process.

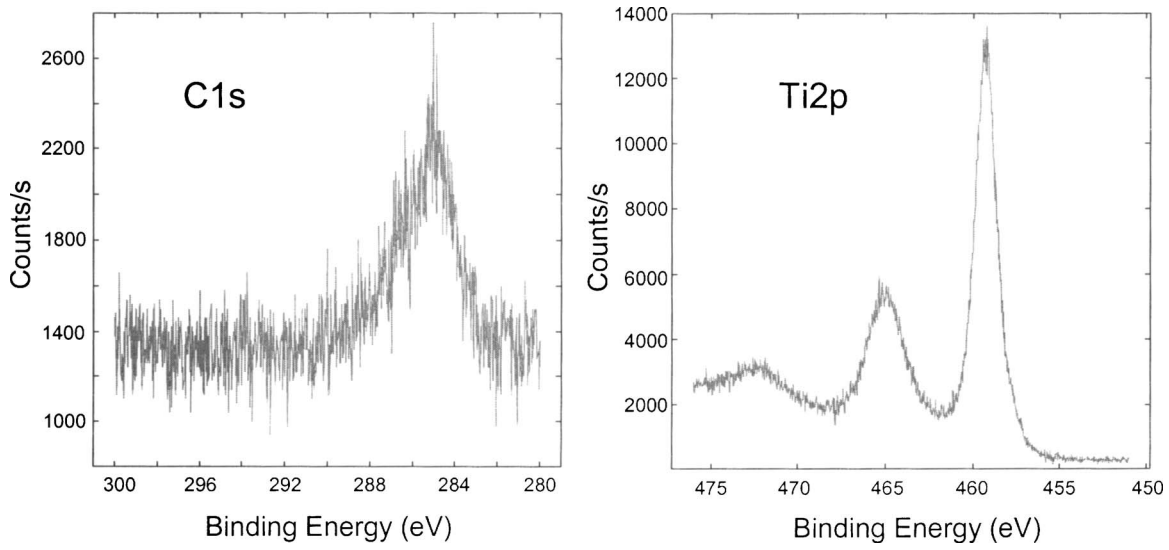

FIG. 4. C 1*s* and Ti 2*p* spectra as obtained from XPS scans on PMMA film post-400 ALD cycles for $TiCl_4$ process.

B. ALD growth studies on PMMA films

Our previous experiments showed that $TiCl_4$ does not nucleate and grow on a PMMA surface as readily as on a Si surface. Therefore, patterned PMMA films were shown to be able to serve as masking layers for area selective ALD. After 100 ALD cycles (2 s [$(TiCl_4)$–25 s(purge)–1 s(H_2O)–60 s(purge)], a titanium concentration of 1.1 at. % was measured on a PMMA surface exposed to the ALD atmosphere. However, 0.7 at. % of Ti was detected on PMMA film surfaces after exposure to 150 pulses of only the $TiCl_4$ precursor [i.e., –2 s($TiCl_4$)–25 s (purge)–]. This indicates that $TiCl_4$ can directly react with the PMMA resin. Chlorine is a highly electronegative atom that significantly reduces electron density on the titanium atom in $TiCl_4$. Thus, the titanium center in $TiCl_4$ behaves as an electron acceptor and functions as a strong Lewis acid. The carbonyl oxygen in PMMA possesses a lone pair of electrons with which $TiCl_4$ can complex or react. In fact, it has been reported that strong Lewis acids (e.g., $AlCl_3$, $TiCl_4$, and $SnCl_4$) can easily complex with carbonyl groups present in acrylates.[20] This reactivity of $TiCl_4$ imparts a limitation on its use as a successful precursor for area selective ALD since it severely limits the types of materials which can serve as nonreactive masking layers. Once TiO_2 nucleates on the PMMA surface, it will serve as an active site for further growth during subsequent ALD cycles. Eventually this will result in deposition of a conformal TiO_2 layer on top of the PMMA film. The presence of such a titania film on the masking layer, which would eventually merge with the titania grown in unmasked areas given a sufficient number of ALD cycles, makes it difficult to remove the PMMA mask after ALD and results in complete loss of pattern definition after a fully conformal film is produced. This means that in order to perform a successful ASALDT process using $TiCl_4$ and PMMA, only a limited number of ALD cycles can be conducted while preventing TiO_2 buildup on the PMMA, which would prevent PMMA removal. For the $TiCl_4$–H_2O–PMMA system, a maximum of ~250 ALD cycles could be run at 160 °C, thus limiting the film thickness attainable. These difficulties with $TiCl_4$ led us to investigate alternative ALD precursors that possess less reactivity toward masking layers such as PMMA.

Metal organic precursors with alkyl or alkoxy groups have been widely investigated as precursors for the deposition of a variety of inorganic oxides including Al_2O_3, HfO_2, ZrO_2, TiO_2, and ZnO. Such ligand groups are not as electronegative as chlorine atoms and thus should not easily cause coordination or reaction with the carbonyl groups found in PMMA. For TiO_2 deposition, titanium isopropoxide is probably the most extensively used precursor among different Ti-alkoxy precursors because of its reasonably high vapor pressure among different Ti-alkoxy precursors.[15] The isopropoxide ligand is also significantly larger than the Cl substituents in $TiCl_4$, and thus access of TiIP to any C═O group in PMMA should be more sterically hindered. As expected, no Ti was detected on PMMA samples exposed only to Ti-isopropoxide pulses. Depositions were conducted on different PMMA samples with successive increases in the number of ALD cycles on different samples. XPS scans of the PMMA samples showed that no Ti was detectable on the polymer surface after 500 ALD cycles (2 s–25 s–2 s–30 s). For comparison, during the same 500 cycles, a 35 nm thick TiO_2 film was deposited on a bare Si substrate.

Figures 4 and 5 show the C 1*s* and Ti 2*p* XPS spectra of the PMMA surface after 400 ALD cycles using $TiCl_4$–H_2O and 500 ALD cycles using $Ti[OCH(CH_3)_2]_4$–H_2O, respectively. As mentioned previously, no Ti is detected when the titanium-isopropoxide precursor was used. In contrast, for the $TiCl_4$ process, a large Ti 2*p* peak is observed due to a TiO_2 layer which has formed on the PMMA film during ALD. Figure 5 presents XPS peak deconvolution results for C 1*s* spectra following ALD using the isopropoxide precursor, where four different peaks corresponding to different C species present in the PMMA film are evident. The peak

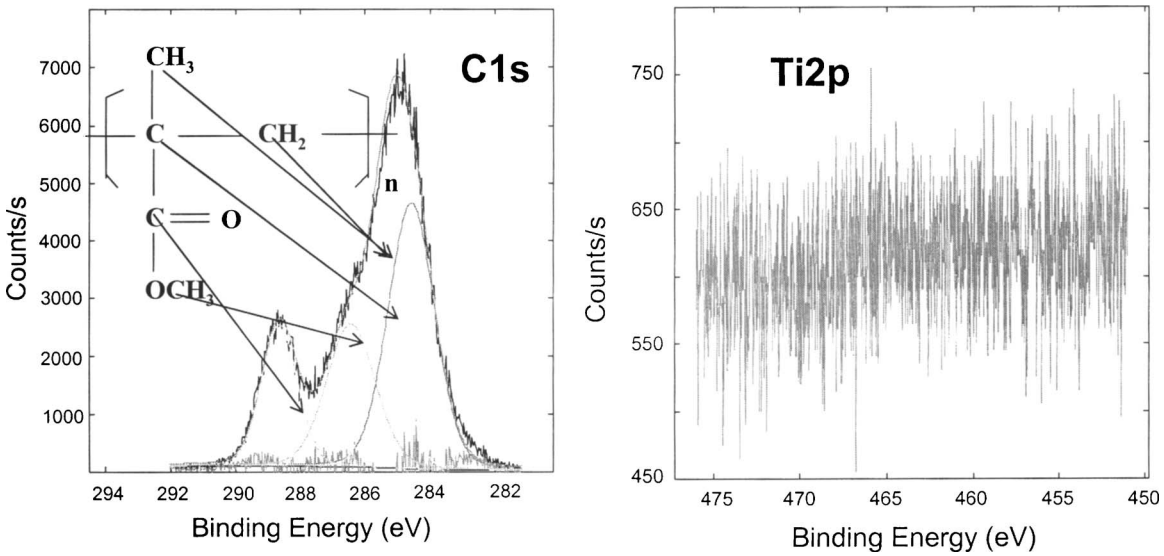

FIG. 5. C 1*s* and Ti 2*p* spectra as obtained from XPS scans on PMMA film post-500 ALD cycles for $Ti[OCH(CH_3)_2]_4$ process.

locations and relative percentage match closely with those reported for standard XPS database spectra from a PMMA polymer. These results further indicate that titanium isopropoxide does not interact with PMMA and that the ALD process does not induce chemical changes in the polymer layer. However, for the $TiCl_4$ process (Fig. 4), a conformal layer of TiO_2 (~25 nm) is deposited on the PMMA surface, and thus only one C 1*s* peak at 284.5 eV is observed which is due to adventitious carbon present on the TiO_2 film. The attenuation length of ejected photoelectrons in XPS is usually 8–10 nm and thus the photoelectrons ejected from the underlying PMMA film (which lies beneath ~25 nm TiO_2 film) are not detected by XPS.

As previously mentioned, it is desirable that the polymer masking layers be easily removed after the ALD process is completed. The PMMA films after TiIP–H_2O ALD were easily removed by rinsing them in acetone (or other solvents for PMMA such as methanol) and DI water. Apparently, the PMMA films simply dissolved in the rinse solvents. In stark contrast, after the $TiCl_4$–H_2O process, the PMMA films were extremely difficult to remove and it was necessary to aid the removal by scratching the film surface at a few locations before washing with warm (T=45 °C) solvent. In this case, PMMA film removal appeared to occur by a lift-off process in which the relatively pure PMMA material at the bottom of the film was dissolved allowing the titanium contaminated PMMA surface layer to lift off and partially dissolve. This clearly suggests that it is desirable to use precursors which do not react with the polymer masking film; otherwise, there is a limit on the number of ALD cycles which can be performed and the ease and cleanliness of the masking film removal process suffer. Optical micrographs showing direct patterned deposition of TiO_2 using the TiIP–H_2O–PMMA-based ASALDT process are presented in Fig. 6. 35 nm thick titania patterns were deposited using 500 ALD cycles (2 s–25 s–2 s–30 s) using lithographically defined patterns in a PMMA film on a Si substrate. As discussed previously, the PMMA film was easily removed after ALD by a simple acetone and DI water rinse. Complete removal of the polymer masking layer from regions around the deposited titania is evident from the optical micrographs. In addition, XPS scans of the TiO_2 patterned structures and the surrounding substrate regions are also shown in Fig. 6. The relative difference in the Ti 2*p* photoelectron intensity from scans on the open and masked regions of the substrate clearly demonstrates the extreme selectivity of the titania deposition. Thus, an improved and simpler ASALDT method than previously reported for the $TiCl_4$–H_2O–PMMA-based approach has been developed and verified.

It is important to note that the results of previous studies which attempted to block ALD nucleation using SAM modified surfaces indicated a direct correlation between surface

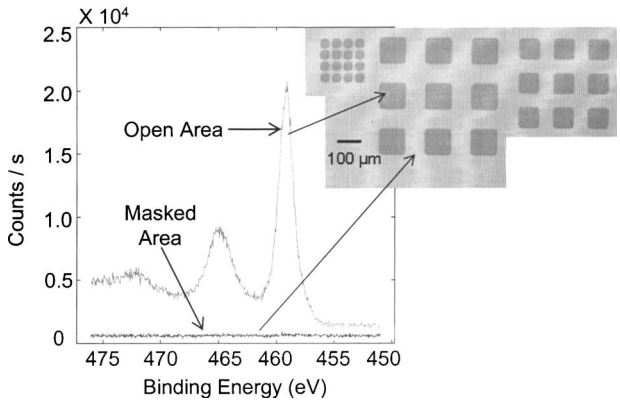

FIG. 6. Comparison of XPS spectra showing the Ti 2*p* peak on a silicon substrate surface after 500 ALD cycles using the TiIP–H_2O precursor system for both surface areas that were covered by a 100 nm PMMA film and for surface areas that were open directly to the ALD atmosphere. Deposition of titania occurred on the open surface while no visible deposition of Ti or titania occurred under the PMMA masked areas. Optical micrographs displaying different size titania patterns deposited using TiIP–H_2O/PMMA ASALDT are also shown.

energy and water contact angle (WCA) of the modified surface with the amount of nucleation observed.[21,22] In the case of studies by Chen *et al.*,[21] it was observed that only octadecyltrichlorosilane and fluorinated-octyltrichlorosilane resulted in sufficiently high water contact angles (109° and 112°, respectively) to successfully block nucleation. Other shorter or branched chain alkyl silanes resulted in lower water contact angles on the masked-area surface, and correspondingly the detected concentration of Hf on these SAM modified regions consistently increased with decreasing SAM surface water contact angle. Similarly, Lee *et al.*[22] observed that the extent of Ti nucleation on mixed SAM surfaces having different surface free energy consistently increased with an increase in surface energy and only the low free energy surface with WCA of 108° showed no nucleation. In general, results in both these studies suggested that a highly hydrophobic masking layer surface ($WCA \geqslant 108°$) was essential to successfully block nucleation on the SAM modified regions. Chen *et al.*[21] also indicated that a high contact angle is only achieved in a well packed monolayer, and that this high degree of packing order is the important feature which prevents ALD precursor access to available reactive sites on the surface. It has also been stated that highly hydrophobic surfaces or low free energy surface also reduce the concentration of physisorbed water on the masking layer surface after each water pulse, and thus can provide lower nucleation as compared to more hydrophilic surfaces. However, this previous work did not clearly identify if one of these two phenomena plays a more dominant role in determining the performance of a SAM surface for selective ALD. The PMMA used in this work has a water contact angle of ~74°, which is significantly lower than that of the SAM surfaces previously reported as being successful for masking ALD processes. The XPS data demonstrate that no Ti is detected on the PMMA surface for 500 ALD cycles when titanium isopropoxide is used as the metallic species precursor. Furthermore, only 30 s of purge after the water pulse was sufficient for successful selective ALD. These results strongly indicate that attainment of selective growth is controlled predominantly by two criteria: (1) the ability of the masking layer to provide a sufficient barrier to the metallic ALD precursor species to prevent it from reaching reactive sites on the substrate surface and (2) the absence of undesired reactions between the masking layer material and the ALD precursors. This blocking of reactive sites on the surface may take the form of a simple diffusional resistance, as is the case of the PMMA films used in this work, or may be due to chemical conversion of reactive sites to a more inert form as is the case with reactive consumption of surface sites by the reactive SAM coatings. Physisorption of water on the masking layer surface appears to play a much less important role and does not appear to pose a serious limitation on the use of less hydrophobic masking layers such as PMMA.

In both the case of SAM coatings and polymer masking layers, an important issue identified in our previous work was the potential ability of ALD precursors to diffuse through the masking layer and reach reactive sites on the substrate surface. Although SAMs in principle reactively passivate the substrate surface, complete elimination of reactive sites on the substrate is essentially impossible. Thus, even the SAM film must act as a diffusion barrier to some extent to successfully prevent nucleation and growth from the substrate on the small number of surface sites which do not react with the silane SAM compounds or from reactive sites created during the SAM deposition process. In the case of physisorbed polymer films, such as the spin cast PMMA materials used in this work, the masking layer does not in principle reactively passivate surface sites but instead acts purely as a diffusion barrier preventing precursor access to the substrate. When using the $TiCl_4-H_2O$ system to deposit titania, a minimum PMMA polymer film thickness on the order of 200 nm was required to prevent nucleation and growth of titania on the substrate surface under the polymer mask. This minimum successful masking layer thickness is consistent with the view of the masking layer as a diffusion barrier. Therefore, even in the case of the titania deposition described in this work, if the titanium precursor has sufficient time to diffuse through the polymer film and reach the silicon substrate, it reacts with surface hydroxyl species and nucleates growth of titania below the polymer film. Subsequently, if water also has sufficient time to diffuse through the polymer film during its pulse, titania growth will occur at the substrate surface beneath the polymer coating. The distance over which a precursor penetrant molecule can diffuse in the polymer film during an ALD precursor exposure cycle is dependent on two factors: (1) the specific time period of the precursor exposure and (2) the diffusion coefficient of the precursor in the polymer. Although the time scale for precursor diffusion can be reduced by reducing the precursor exposure cycle time, this can result in subsaturation precursor exposure of the surface leading to submonolayer growth in the desired areas. This in turn leads to lower ALD growth rates and overall longer ALD times due to the added ALD cycles needed to obtain the same deposition thickness. Therefore, in order to produce successful masking layers and area selective deposition processes, it is prudent to adjust the masking layer film thickness with a knowledge of the diffusion coefficient of the ALD precursors in the masking films to optimize the process.

The ability to adjust the polymer masking layer film thickness for a given polymer-precursor system to produce successful passivation of the substrate surface was demonstrated in our previous work on titania deposition using the $TiCl_4-H_2O$ precursor system.[10] A series of depositions was conducted on PMMA samples of different thicknesses and the amount of titania growth under the polymer film was assessed. After 100 ALD cycles [2 s($TiCl_4$)–25 s(N_2)–1 s(H_2O)–60 s(N_2)], the polymer film was removed using acetone and the underlying substrate surfaces analyzed by XPS. First, it was observed in the case of thicker PMMA films (180 and 420 nm) that the polymer films were removed easily by dipping the samples in acetone. However, in the case of thinner films (32, 56, and 103 nm) it was necessary to assist the removal process by

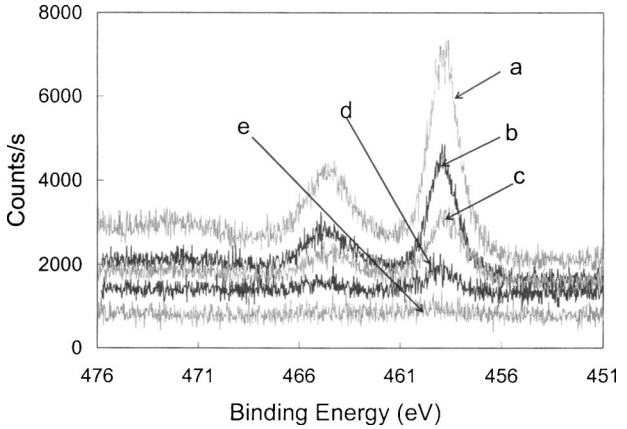

FIG. 7. XPS spectra showing the Ti 2*p* peak measured on the silicon substrate after 100 ALD cycles [2 s($TiCl_4$)–25 s(N_2)]-1 s[(H_2O)–60 s(N_2)] for different initial thicknesses of the PMMA masking film. The scans were taken after the PMMA film was removed from the silicon wafer. PMMA film thicknesses were (a) 32 nm, (b) 56 nm, (c) 103 nm, (d) 180 nm, and (e) 420 nm. The spectra have been shifted vertically along the *Y* axis arbitrarily for purposes of separation and clearer representation.

physically wiping the film off the substrate in the presence of solvent. This difficulty in removing the thinner films suggested that reaction and deposition of titania occurred at the substrate-polymer interface. XPS scans were performed on the samples after polymer removal to measure the total Ti content on the surface. Figure 7 shows the Ti 2*p* peak on the surface of samples after polymer removal for different initial thicknesses of the PMMA layer. Clearly, detectable Ti deposition was observed in the case of the thinner polymer samples while no Ti deposition was detectable on the 420 nm thick samples and very little deposition was visible on the 180 nm thick polymer film sample. In addition, the amount of Ti detected scales with polymer film thickness. This is consistent with the fact that the precursor diffuses through the polymer and reacts at the substrate interface since higher concentrations of precursor will be present at the substrate surface in the case of thinner polymer films. It is also observed that the location for the Ti 2*p*3 peak obtained for the 180 nm thick polymer film sample [spectra (d)] appears at a binding energy of 459.0 eV, which is 0.2 eV higher than the 458.8 eV Ti 2*p*3 peak location (characteristic of titanium atoms in TiO_2) obtained with the other thinner samples. This shift in the peak location can be attributed to differences in the chemical environment of the titanium atoms. As discussed previously, significantly fewer $TiCl_4$ molecules reach the polymer-substrate interface in the 180 nm thick polymer films as compared to the cases of the thinner films. Thus, the titania layer formed below the 180 nm thick polymer film after the 100 ALD cycles possesses a greater fraction of titanium atoms involved in Ti–O–Si bonds (which are the first layer of bonds formed at the substrate interface) with respect to the overall content of titanium atoms. As the masking layer thickness is reduced, a larger amount of titania is grown under the polymer film resulting in a higher fraction of titanium atoms involved in Ti–O–Ti bonds with respect to the overall titanium atom content. Thus, in the thinner polymer film samples the observed Ti 2*p*3 peak location is located closer to the characteristic Ti 2*p*3 location for pure TiO_2 films. XPS scans on Si surfaces exposed to only one and two pulses of $TiCl_4$ also exhibited Ti 2*p*3 peaks located at 459.0 eV which are assumed to be due to the presence of mainly Ti–O–Si in these samples. This observation further supports the idea that the observed 0.2 eV shift in the Ti 2*p*3 peak for the 180 nm thick polymer film sample shown in Fig. 7 is due to the slightly different chemical environment of the majority of titanium atoms in the extremely thin titania layer formed in that case.

These results suggested that selection of a minimum film thickness for the polymer masking layer is required for a specific polymer-precursor-cycle time combination. In the $TiCl_4$–H_2O–PMMA PM-ASALDT process, a minimum masking layer thickness of approximately 200 nm is required to avoid titania growth under the polymer surface.

In the case of the TiIP–H_2O system used in the current work, the TiIP precursor is significantly larger than the $TiCl_4$ precursor used previously. Both Ti precursors are larger than the water molecules used as the oxidizing agent in both cases, and thus diffusion of the Ti precursor is expected to be the limiting step in titania growth under the polymer film. Therefore, it is expected that the minimum PMMA masking layer thickness for TiIP–H_2O should be significantly smaller than in the $TiCl_4$–H_2O case. A series of depositions on silicon substrates was conducted with different PMMA film thicknesses using the TiIP–H_2O precursor system to investigate the effect of precursor size on diffusion through the polymer film. After ALD, the polymer film was removed and XPS of the resultant surface was performed to quantify titania deposition under the polymer film. It was observed that the thickness of PMMA could be reduced to ~10 nm without detection of TiO_2 deposition on the substrate beneath the polymer film. Attempts to form PMMA films thinner than 10 nm were unsuccessful due to dewetting phenomena.[23,24] A rough estimate of the mean molecular diameter for titanium isopropoxide and titanium tetrachloride can be estimated from the density and molecular mass of the corresponding liquids.[25,26] The calculations indicate that the mean molecular diameters for titanium tetrachloride and titanium isopropoxide are approximately 0.57 and 0.79 nm, respectively. This suggests that a titanium-isopropoxide molecule is ~2.73 times the volume of a titanium tetrachloride molecule. At present no data are available that allow a direct comparison of the diffusion coefficients and solubilities of these penetrants in PMMA at 160 °C. However, Berens and Hopfenberg[25] investigated gas and vapor diffusivities in PMMA at 90 °C, and their results suggest that the order of magnitude of the penetrant diffusion coefficient in the polymer drops linearly with penetrant mean diameter for spherical molecules. Based on the results presented by Berens and Hopfenberg, it can be estimated that the diffusivity of TiIP is more than six orders of magnitude smaller than $TiCl_4$ diffusivity if the diffusion behavior of PMMA at 160 °C is similar to that at 90 °C. However, it is important to note that PMMA at 160 °C is above its glass transition temperature

(T_g) and thus is in its rubbery state. The penetrant diffusivity in a rubbery polymer is generally known to be a less strong a function of penetrant size relative to that in the glass.[27] Vrentas *et al.*[28] predicted diffusion coefficients of trace solvents in polystyrene at various temperatures above and below its T_g and observed similar behavior. Extending the results presented in their study to the penetrant size difference corresponding to our work for TiIP versus $TiCl_4$ and accounting for the increase in temperature beyond the T_g of PMMA, we estimate that there is at least three to four orders of magnitude difference between the diffusion coefficients of $TiCl_4$ and TiIP in PMMA at 160 °C. If diffusion of the precursors in the PMMA film can be described as a Fickian diffusion process, the distance covered by the penetrant molecule scales with square root of the product of the penetrant diffusivity and diffusion time (i.e., $L \propto \sqrt{Dt}$). Therefore, for two penetrants that differ in diffusion coefficient by three orders of magnitude such as the case of $TiCl_4$ and TiIP, the diffusion distance of the slower diffusing penetrant (TiIP) would be expected to be ~30 times less than that of the faster diffusing penetrant ($TiCl_4$) for the same diffusion time. This roughly translates into a minimum masking layer thickness of 30 times less for TiIP as compared to $TiCl_4$. Based on the 200 nm minimum effective masking layer thickness for $TiCl_4$, this analysis suggests that a masking layer thickness of ~6 nm should be sufficient in the case of TiIP. This prediction is consistent with the observation that no titania deposition was detected on the Si substrate surface for PMMA film thicknesses down to 10 nm. As previously mentioned, ALD on PMMA film thicknesses equal to 5 nm and lower was also attempted. However, such polymer thin films displayed dewetting when heated and some films showed the presence of pinholes when scanned under atomic force microscopy immediately after spin coating. Therefore ALD precursor diffusion studies on films thinner than 10 nm were not possible.

One of the advantages of using polymer films as masking layers is that conventional and commercially established optical lithography techniques can be easily used to pattern these masks. The resolution and depth of focus for a given optical lithography system can be described by the following equations:

$$\text{resolution} = k\frac{\lambda}{\text{NA}}, \tag{1}$$

$$\text{depth of focus} = \pm\frac{\lambda}{2\text{NA}^2}. \tag{2}$$

As the resolution of optical lithography tools continues to increase by decreasing the exposure wavelength and increasing the numerical aperture of the lens systems, the depth of focus for such tools is reduced. This leads to a reduction in the thickness of the resist films used in the fabrication process. According to the ITRS roadmap,[29] the required resist thicknesses will be in the range of 120–160 nm by the year 2010 (45 nm node) and 50–80 nm by 2016 (22 nm node). However, the new TiIP–H_2O process presented in this work has shown the ability to be utilized in conjunction with polymer film thicknesses well below these optical lithography thickness requirements. Thus, by choosing combinations of optical resist polymers and precursors which display low precursor diffusivities in the masking layer and low reactivities toward one another, area selective ALD at essentially the resolution limits of the high throughput optical lithography patterning technologies should be possible. Obviously PMMA is not an ideal choice for high volume manufacturing using optical lithography due to its relatively low sensitivity to ultraviolet light, and therefore work is currently in progress to develop high photospeed photodefinable masking layers for use with UV optical lithography tools. However, the PMMA process demonstrated in this work is a good choice for extremely high resolution electron beam lithography-based production of titania nanopatterns.

IV. CONCLUSIONS

Area selective ALD of titanium dioxide has been investigated and compared using two different precursors, $TiCl_4$ and $Ti[OCH(CH_3)_2]_4$, in conjunction with PMMA as a photodefinable polymer masking layer. Inherent reactivity of the precursors with the masking layer and diffusion of the ALD precursors through the masking layer have clearly been shown to be two critical characteristics in the design of a successful polymer masked-area selective ALD (PMASALDT) process. It is believed that $TiCl_4$ can coordinate with the C═O bond present in PMMA since it is a strong Lewis acid, thus allowing reaction and nucleation of TiO_2 on PMMA. In contrast, titanium isopropoxide was virtually unreactive towards PMMA and thus no Ti was detected on PMMA surfaces even after 500 ALD cycles using the TiIP–H_2O precursor system. This negligible reactivity between TiIP and PMMA allows the PMMA masking film to be easily removed after ALD using simple solvent washes. The experimental results also indicate that extreme hydrophobicity of the masked surface may not be as critical a prerequisite for successful polymer masking-based selective ALD as it has been reported previously for SAM-based area selective ALD processes (e.g., a minimum water contact angle on the masking surface greater than 109° was reported previously[21,22]). The larger size of the titanium-isopropoxide precursor molecule slows its diffusion through PMMA films as compared to $TiCl_4$, and thus allows the use of much thinner polymer masking layers for TiIP–H_2O as compared to $TiCl_4$–H_2O. A PMMA masking layer film thickness of approximately 10 nm was effective for masking the TiIP–H_2O system while a PMMA film at least 180–200 nm thick was required to avoid titania deposition under the polymer film for the $TiCl_4$–H_2O system. These results suggest that the intrinsic reactivity of the polymer resin with the ALD precursors, the presence of remnant precursors in the polymer film after each precursor pulse, and diffusion of precursor through the masking layer are the critical parameters which must be considered in establishing a successful polymer mask-based area selective ALD process. Overall, the use of

the TiIP–H_2O–PMMA system has been shown to be a good first example of a lithographically compatible area selective deposition process for titania.

[1]M. Ritala and M. Leskela, *Handbook of Thin Film Materials* (Academic Press, San Diego, CA, 2002), Vol. 1, p. 103–159.
[2]M. Leskela and M. Ritala, Angew. Chem., Int. Ed. **42**, 5548 (2003).
[3]R. Chen, H. Kim, P. C. McIntyre, D. W. Porter, and S. F. Bent, Appl. Phys. Lett. **86**, 191910 (2005).
[4]R. Chen, H. Kim, P. C. McIntyre, and S. F. Bent, Appl. Phys. Lett. **84**, 4017 (2004).
[5]M. Yan, Y. Koide, J. R. Babcock, P. R. Markworth, J. A. Belot, T. J. Marks, and R. P. H. Chang, Appl. Phys. Lett. **79**, 1709 (2001).
[6]J. P. Lee and M. M. Sung, J. Am. Chem. Soc. **126**, 28 (2004).
[7]M. H. Park, Y. J. Jang, H. M. Sung-Suh, and M. M. Sung, Langmuir **20**, 2257 (2004).
[8]A. Sinha, D. W. Hess, and C. L. Henderson, Proc. SPIE **5753**, 476 (2005).
[9]K. J. Park, J. M. Doub, T. Gougousi, and G. N. Parsons, Appl. Phys. Lett. **86**, 051903 (2005).
[10]A. Sinha, D. W. Hess, and C. L. Henderson, J. Electrochem. Soc. **153**, G465 (2006).
[11]K. Prabhakaran, Y. Kobayashi, and T. Ogino, Surf. Sci. **290**, 239 (1993).
[12]XPS Handbook, PHI Electronics.
[13]A. Rahtu and M. Ritala, Chem. Vap. Deposition **8**, 21 (2002).
[14]H. Doring, K. Hashimoto, and A. Fujishima, Ber. Bunsenges. Phys. Chem. **96**, 620 (1992).
[15]M. Ritala, M. Leskela, L. Niinisto, and P. Haussalo, Chem. Mater. **5**, 1174 (1993).
[16]J. Aarik, A. Aidla, T. Uustare, M. Ritala, and M. Leskela, Appl. Surf. Sci. **161**, 385 (2000).
[17]R. Matero, A. Rahtu, and M. Ritala, Chem. Mater. **13**, 4506 (2001).
[18]J. Aarik, A. Aidla, V. Sammelselg, H. Siimon, and T. Uustare, J. Cryst. Growth **169**, 496 (1996).
[19]R. L. Puurunen, Chem. Vap. Deposition **11**, 79 (2005).
[20]X. Assfeld, J. Garcia, J. I. Garcia, J. A. Mayoral, M. G. Proietti, M. F. Ruiz-Lopez, and M. C. Sanchez, J. Chem. Soc., Chem. Commun. 2165 (1994).
[21]R. Chen, H. Kim, P. C. McIntyre, and S. F. Bent, Chem. Mater. **17**, 536 (2005).
[22]J. P. Lee, Y. J. Jang, and M. M. Sung, Adv. Funct. Mater. **13**, 873 (2003).
[23]G. Reiter, Phys. Rev. Lett. **68**, 75 (1992).
[24]K. M. Ashley, D. Raghavan, J. F. Douglas, and A. Karim, Langmuir **21**, 9518 (2005).
[25]A. R. Berens and H. B. Hopfenberg, J. Membr. Sci. **10**, 283 (1982).
[26]*CRC Handbook of Chemistry and Physics*, 63rd ed. (CRC, Boca Raton, FL, 1982), p. B-159 and C-721.
[27]W. J. Koros and M. W. Hellums, *Encyclopedia of Polymer Science and Engineering*, 2nd ed. (Wiley, New York, 1990), Vol. Suppl., p. 724–802.
[28]J. S. Vrentas, H. T. Liu, and J. L. Duda, J. Appl. Polym. Sci. **25**, 1297 (1980).
[29]International Technology Roadmap for Semiconductors, 2003.